# Novel cGMP Efflux Inhibitors Identified by Virtual Ligand Screening (VLS) and Confirmed by Experimental Studies

Georg Sager,[†] Elin Ø. Ørvoll,[†] Roy A. Lysaa,[†] Irina Kufareva,[‡] Ruben Abagyan,[‡] and Aina W. Ravna*[,†]

[†]Medical Pharmacology and Toxicology, Department of Medical Biology, Faculty of Health Sciences, University of Tromsø, 9037 Tromsø, Norway

[‡]Skaggs School of Pharmacy and Pharmaceutical Sciences, University of California—San Diego, 9500 Gilman Drive, La Jolla, California 92093, United States

**ABSTRACT:** Elevated intracellular levels of cyclic guanosine monophosphate (cGMP) may induce apoptosis, and at least some cancer cells seem to escape this effect by increased efflux of cGMP, as clinical studies have shown that extracellular cGMP levels are elevated in various types of cancer. The human ATP binding cassette (ABC) transporter ABCC5 transports cGMP out of cells, and inhibition of ABCC5 may have cytotoxic effects. Sildenafil inhibits cGMP efflux by binding to ABCC5, and in order to search for potential novel ABCC5 inhibitors, we have identified sildenafil derivates using structural and computational guidance and tested them for the cGMP efflux effect. Eleven compounds from virtual ligand screening (VLS) were tested in vitro, using inside-out vesicles (IOV), for inhibition of cGMP efflux. Seven of 11 compounds predicted by VLS to bind to ABCC5 were more potent than sildenafil, and the two most potent showed $K_i$ of 50−100 nM.
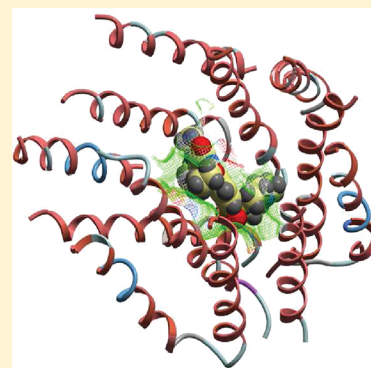
## ■ INTRODUCTION

Clinical studies have shown that extracellular cyclic guanosine monophosphate (cGMP) levels are elevated in various types of cancer.[1−4] The human ATP binding cassette (ABC) transporter ABCC5 transports cGMP out of cells,[5] and the increased cGMP efflux from cancer cells may be caused by an up-regulation of ABCC5. cGMP regulates several apoptosis-associated genes, and intracellular elevation of cGMP concentration by inhibition of ABCC5 efflux may give cytotoxic effects.[6]

ABCC5 belongs to the ABC transporters, which are structurally related membrane proteins featuring intracellular motifs that exhibit ATPase activity.[7] This nucleotide binding domain (NBD), which contains the Walker A and Walker B motifs, cleaves ATP's terminal phosphate to energize the transport of substrate molecules against a concentration gradient. ABC genes are highly conserved within species, indicating that these genes may have been present since the beginning of eukaryotic evolution.[7,8] The overall topology of ABCC5 is divided into transmembrane domain (TMD) 1-NBD1-TMD2-NBD2.

No X-ray crystal structure of ABCC5 has been reported, but molecular models of ABCC5 may be constructed by homology using a known 3D crystal structure of an evolutionary related protein as a template. Docking, which is a method that suggests the preferred orientation of a drug molecule in the binding site of a drug target, can be used to predict the binding poses of substrates, known inhibitors, and drug candidates to ABCC5, while the subsequent process of scoring can help rank-order them. In virtual ligand screening (VLS), drug candidates from compound databases can be selected using computer programs to theoretically predict whether they bind to ABCC5 using an ABCC5 model.

We have previously presented models of ABCB1,[9,10] ABCC4,[10,11] and ABCC5[10,12] in outward-facing conformations and inward-facing conformations based on the *Staphyllococcus aureus* ABC transporter Sav1866,[13] which has been crystallized in an outward-facing ATP-bound state, and on the *Escherichia coli* MsbA, which has been crystallized in a wide open inward-facing conformation.[14] Here we present a homology model of ABCC5 based on the X-ray crystal structure of the *Mus musculus* ABCB1 in a drug-bound conformation.[15] ABCC5 efflux is inhibited by the phosphodiesterase 5 (PDE5) inhibitor sildenafil,[5] and in order to search for potential ABCC5 inhibitors, the ABCC5 model was used for VLS of sildenafil derivates. The template resolution was low (4.4 Å), and the amino acid sequence identity between *Mus musculus* ABCB1 and the human ABCC5 is 24%, clearly implying that the ABCC5 homology model has elements of uncertainty.

The aim of this study was to use structural and computational guidance to create chemical diversity around sildenafil and test it for the cGMP efflux effect. The methodologies of ligand-based drug design, which relies on knowledge of other molecules that bind to the biological target of interest, and structure-based drug design, which is based on knowledge about the three-dimensional structure of the biological target, were combined, searching for sildenafil analogues in databases and using the ABCC5 model as an additional filter to select compounds to test for binding to ABCC5 in vitro. Eleven compounds from the VLS, which were selected based on score and drug likeness, were tested in vitro for a modulation of ABCC5 activity.

## ■ RESULTS

**In Silico.** The energy minimized ABCC5 model is shown in Figure 1. The model was in an inward-facing conformation with
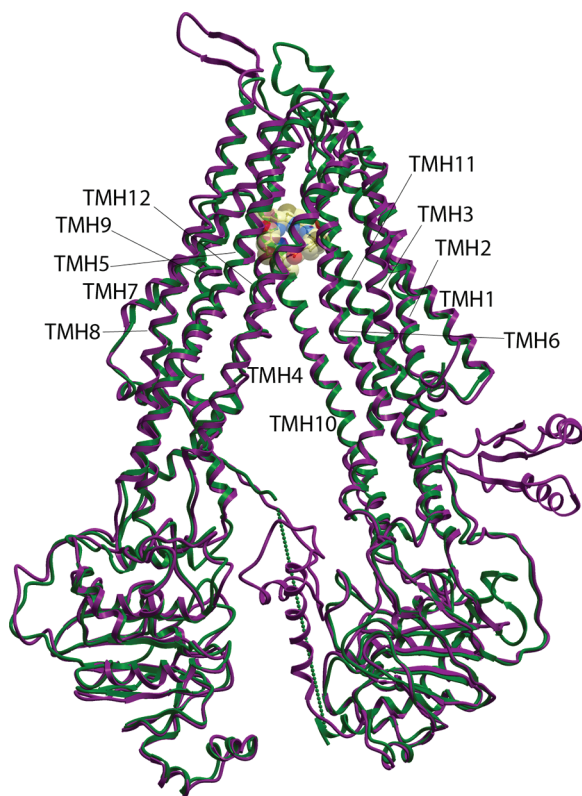


**Figure 1.** Superimposition of the energy minimized ABCC5 model (purple) and the template X-ray crystal structure of the *Mus musculus* ABCB1[15] (green). The green dotted line of template indicates the missing loop connecting NBD1 and TMD2. The ligand QZ59-RRR cocrystallized with *Mus musculus* ABCB1[15] is shown in space-filling solid style.

the NBDs separated by approximately 18 Å. A large internal cavity open to the cytoplasm was formed by two transmembrane helix (TMH) bundles: TMHs 1, 2, 3, 6, 10, 11 and TMHs 4, 5, 7, 8, 9, 12. Key amino acid residues located in the large internal putative drug binding cavity included Gln190 (TMH1),

Val411 (TMH5), Asn441, Thr444 and Lys448 (TMH6), Ser872 (TMH7), and Gln1138 (TMH12). The Walker A motifs consisted of a coiled loop and a short α-helix (P-loop), and the Walker B motifs were in β-sheet conformation and localized in the NBD's hydrophobic cores, which were constituted of five parallel β-sheets and one antiparallel β-sheet. The loop connecting NBD1 and TMD2 of the model featured three α-helices in the region between His767 and Val817, while in the region between Lys818 and Val841 it was in an extended conformation. However, it should be kept in mind that this loop was not present in the template and that modeling loops of this lengths is relatively inaccurate, and consequently the modeled loop structures must be regarded as uncertain. The loop is approximately 40 Å from the binding pocket, and accordingly, the inclusion of this loop may not be necessary for the purpose of this study.

The Errat option of the Stuctural Analysis and Verification Server (SAVES) http://nihserver.mbi.ucla.edu/SAVES/ reported that the overall quality factor of the ABCC5 model was 91.7, and a value above 90 indicates a good model. According to the Ramachandran plot provided by the Procheck option, 80.1% of the ABCC5 residues were in the most favored regions, 14.8% were in additional allowed regions, 2.5% were in generously allowed regions, and 2.6% were in disallowed regions. The summary of the Whatcheck option reported that the ABCC5 model was satisfactory.

The best docking score of the known binders was −29.5 kcal/mol, and this value was used as a threshold score for the VLS. Figure 2 shows sildenafil docked into the binding site of ABCC5. Thirty compounds in the VLS had a better score than the threshold score of −29.5 kcal/mol, the best one being −37.9 kcal/mol. Table 1 shows the potential ABCC5 inhibitors from the VLS that were ordered from Ambinter. Docking revealed a tendency where the guanine-like moiety of the ligands interacted with Gln190 (TMH1) of ABCC5. Of the three binding site conformations included in the 4D docking procedure, the two conformations with the lowest energies were the conformations generally preferred by the ligands.

**In Vitro.** A single concentration (32 μM) of the compounds shown in Figure 3 was tested for their ability to inhibit [³H]cGMP uptake into inside-out vesicles (IOV). Sildenafil was introduced as a reference inhibitor, and the effect of the well-known PDE5 inhibitors (zaprinast and dipyridamole) was also determined. Figure 3 shows that sildenafil inhibited 85% of cGMP uptake.
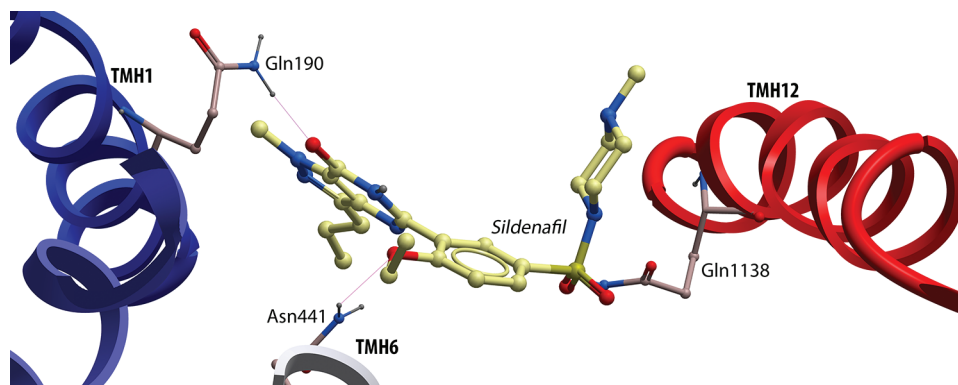


**Figure 2.** Sildenafil docked into the binding site of ABCC5 viewed from the extracellular side. Amino acids with hydrogen bond interactions with sildenafil are displayed as sticks colored according to atom type (C = light yellow; H = gray; O = red; N = blue; sulfur = yellow): Gln190 (TMH1), Asn441 (TMH6), and Gln1138 (TMH12).

The corresponding values for zaprinast and dipyridamole were approximately 95%. However, several of the compounds brought forward by VLS showed even higher potency than sildenafil. Compounds **1** and **2** blocked the transport completely, whereas compounds **3**, **4**, **5**, **6**, and **7** inhibited transport more effectively than the starting point molecule sildenafil.

**Table 1. Potential ABCC5 Inhibitors from the VLS That Were Ordered from Ambinter, with Compound Code, IUPAC Name, Pubchem Compound ID, ICM Druglikeness Score (Predicted Based on 5000 Marketed Drugs from WDI (Positives) and 10 000 Nondrug Compounds (Negatives)), ICM Docking Score, % of cGMP Efflux, and $K_i$**
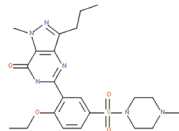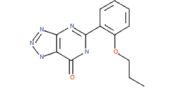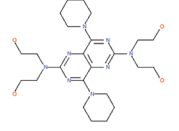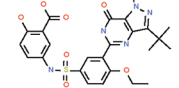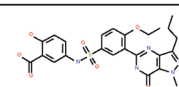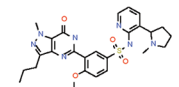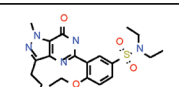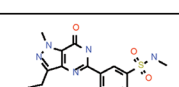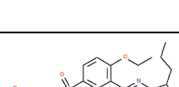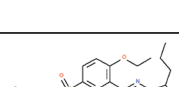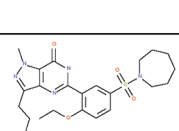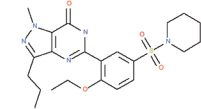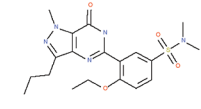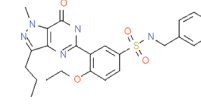
| Compound | Ambinter compound code | IUPAC name | Pubchem compound ID | Molecular structure | Drug likeness | ICM Score | % cGMP efflux | Ki (nM) |
|---|---|---|---|---|---|---|---|---|
| Sildenafil | | 5-[2-ethoxy-5-(4-methylpiperazin-1-yl)sulfonylphenyl]-1-methyl-3-propyl-4H-pyrazolo[4,3-d]pyrimidin-7-one | CID 5212 | | 0.9335 | -23.55 | 16.2 | 1200 ± 170 |
| Zaprinast | | 5-(2-propoxyphenyl)-2,3-dihydrotriazolo[4,5-d]pyrimidin-7-one | CID 5722 | | 0.4367 | -19.61 | 5.7 | |
| Dipyridamole | | 2-[[2-[bis(2-hydroxyethyl)amino]-4,8-di(piperidin-1-yl)pyrimido[5,4-d]pyrimidin-6-yl]-(2-hydroxyethyl)amino]ethanol | CID 3108 | | 0.7904 | -19.08 | 5.9 | |
| 1 | STOCK3S-39213 | 5-[[3-(3-tert-butyl-1-methyl-7-oxo-4H-pyrazolo[4,3-d]pyrimidin-5-yl)-4-ethoxyphenyl]sulfonylamino]-2-hydroxybenzoic acid | CID 1598490 | | 0.7573 | -30.93 | 0 | 75.3 ± 3.1 |
| 2 | STOCK1S-60049 | 5-[[4-ethoxy-3-(1-methyl-7-oxo-3-propyl-4H-pyrazolo[4,3-d]pyrimidin-5-yl)phenyl]sulfonylamino]-2-hydroxybenzoic acid | CID 1899750 | | 1.064 | -29.06 | 0 | 65.3 ± 6.4 |
| 3 | PHAR099048 | 4-ethoxy-3-(1-methyl-7-oxo-3-propyl-4H-pyrazolo[4,3-d]pyrimidin-5-yl)-N-[3-(1-methylpyrrolidin-2-yl)pyridin-2-yl]benzenesulfonamide | CID 4921527 | | 1.246 | -32.33 | 5.5 | |
| 4 | STOCK1S-59261 | 4-ethoxy-N,N-diethyl-3-(1-methyl-7-oxo-3-propyl-4H-pyrazolo[4,3-d]pyrimidin-5-yl)benzenesulfonamide | CID 1899174 | | 0.3768 | -31.02 | 6.1 | |
| 5 | STOCK1S-52373 | 4-ethoxy-N-methyl-3-(1-methyl-7-oxo-3-propyl-4H-pyrazolo[4,3-d]pyrimidin-5-yl)benzenesulfonamide | CID 1896380 | | 0.2554 | -31.24 | 5.5 | |
| 6 | STOCK1S-62278 | 4-ethoxy-N-(2-hydroxyethyl)-3-(1-methyl-7-oxo-3-propyl-4H-pyrazolo[4,3-d]pyrimidin-5-yl)benzenesulfonamide | CID 1900265 | | 0.3706 | -30 | 8.1 | |
| 7 | STOCK1S-53050 | 4-ethoxy-N-(2-hydroxyethyl)-N-methyl-3-(1-methyl-7-oxo-3-propyl-4H-pyrazolo[4,3-d]pyrimidin-5-yl)benzenesulfonamide | CID 1896597 | | 0.5718 | -31.47 | 12.0 | |
| 8 | STOCK1S-57138 | 5-[5-(azepan-1-ylsulfonyl)-2-ethoxyphenyl]-1-methyl-3-propyl-4H-pyrazolo[4,3-d]pyrimidin-7-one | CID 1897952 | | 0.7381 | -31.98 | 22.0 | |

**Table 1. continued**

| 9 | STOCK1S-53798 | 5-(2-ethoxy-5-piperidin-1-ylsulfonylphenyl)-1-methyl-3-propyl-4H-pyrazolo[4,3-d]pyrimidin-7-one | CID 1896867 | | 0.9196 | -29.64 | 37.1 | |
| 10 | STOCK1S-68740 | 4-ethoxy-N,N-dimethyl-3-(1-methyl-7-oxo-3-propyl-4H-pyrazolo[4,3-d]pyrimidin-5-yl)benzenesulfonamide | CID 1902581 | | 0.3803 | -34.62 | 37.7 | |
| 11 | STOCK1S-53657 | N-benzyl-4-ethoxy-3-(1-methyl-7-oxo-3-propyl-4H-pyrazolo[4,3-d]pyrimidin-5-yl)benzenesulfonamide | CID 1896826 | | 0.5251 | -34.76 | 49.6 | |



**Figure 3.** The sildenafil-like substances were selected by criteria described in Experimental Section. They were tested for their ability to inhibit ATP-dependent high affinity transport of [³H]cGMP (3.3 μM). A single inhibitor concentration (32 μM) approximately 10 times above the concentration of [³H]cGMP was employed to unveil the most potent inhibitors. In addition, sildenafil, zaprinast, and dipyri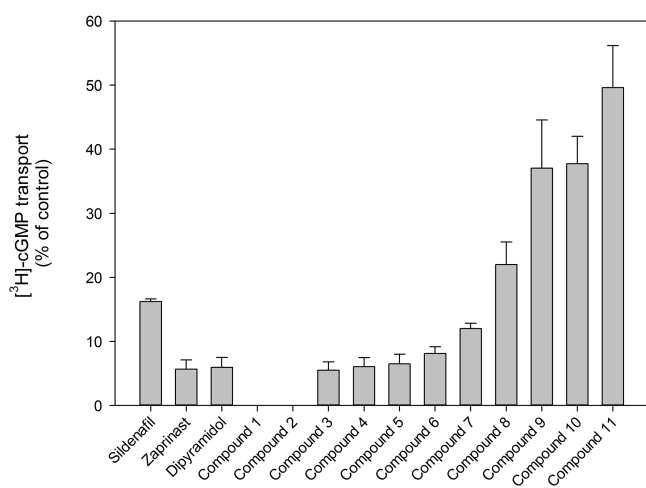damole were included as positive controls. Unpaired $t$ test with Welch correction was performed and showed that all substances were statistically significantly different ($p < 0.05$), either more potent or less potent than sildenafil, with the exception of compounds **8** and **9**. The results are presented as mean value + SEM.

$K_i$ values of the most potent inhibitors of cGMP transport where calculated, and while sildenafil, which was used as reference inhibitor, showed a $K_i$ of 1200 ± 170 nM, the corresponding values of compounds **1** and **2** were 75.3 ± 3.1 and 65.3 ± 6.4 nM, respectively.

## ■ DISCUSSION

In this study, molecular modeling techniques were used for construction of an ABCC5 model and for identification of its interactions with sildenafil derivates. Molecular modeling and docking may help to elucidate molecular interactions between drugs and drug targets, aiding the search to understand the intermolecular forces involved in determining the potency and the specificity of the drug. However, homology modeling of

transporters must be regarded with caution; there are few templates available, if any, and they often have low resolution, and homology between the target transporter and the template may also be low. The sequence identity between target and template in the present study was relatively low (24%), so even though a multiple sequence alignment, which highlights evolutionary relationships and increases the probability that corresponding sequence positions are correctly aligned, was used to guide the homology modeling procedure, the low homology gives elements of uncertainty to the resulting model. Homology modeling of membrane transporters often implies low homology; the sequence identity between the frequently used template *Aquifex aeolicus* leucine tranporter LeuT$_{Aa}$ and modeled monoamine transporters is ~20%,[16] and the sequence identities in the transmembrane regions between the G-protein-coupled receptors and bacteriorhodopsin are 6−11%, even though their TMH arrangement is the same.[17] The quality of the template must also be considered, both in regard to low resolution and in regard to the fact that the amphiphilic nature of membrane proteins causes difficulties in experimental structure determination. Thus, even when crystallization is successful, the protein is no longer in its natural environment, and conformational disruption of the transporter due to the presence of detergent molecules during crystallization cannot be excluded. Interestingly, recent cysteine cross-linking studies, linking residues in TMH3 and TMH9 of ABCB1[18] and between residues in the C-terminal ends of the two NBDs of ABCB1,[19] have shown that ABCB1 still functions when covalently cross-linked. This indicates that the Sav1866 X-ray crystal structure,[13] which is in an outward-facing conformation, may also serve as a template for modeling and running VLS on ABCC5 and may also yield interesting inhibitors.

Structural flexibility was taken into account when performing docking and VLS on the ABCC5 model. A crystal structure of a transporter may not be a realistic representation of the transporter in its native form, and transporters may undergo substantial conformational changes during the transport cycle. Large ranges of motion, changing the accessibility of the transporter from a cytoplasmic (inward) facing conformation to an extracellular (outward) facing conformation, have been revealed from X-ray crystal structures of the bacterial ABC transporter lipid flippase, MsbA, trapped in different conformations.[14] Induced fit, which has been demonstrated in a cysteine-scanning

mutagenesis and oxidative cross-linking study of substrate-induced changes in ABCB1[20] and conformational changes due to transport, may be an important part of ligand recognition. The energy-based torsional sampling ("fumigation") generated additional conformations of the ligand binding area of ABCC5, with lower energies than the starting model. Of the three conformations used for docking and VLS, the two lowest energy conformations were preferred by the ligands, indicating that these conformations were more "druggable". The 4D docking, where the ligands are free to "choose" their preferred binding site conformation, may be viewed as a theoretical model of how the ligand is attracted to the drug target in a relatively more active conformation. Insight into structural changes of the drug target for yielding a lower energy drug−drug target complex may elucidate how the conformation of the binding site contributes to the adoption of an energetically favorable complex. Ideally, these observations can aid prediction of how a designed drug will fit into the drug target.

In an interdisciplinary approach combining in silico studies (theoretical molecular modeling) and in vitro studies (experimental pharmacology), the ABC transporter model may be considered as a working tool for generating hypotheses and designing further experimental studies related to ABC transporter structure and function and their ligand interactions. In vitro studies and transporter modeling are complementary to each other in an iterating process toward a better understanding of the structure and function of these proteins. The VLS add-on to the internal coordinate mechanics (ICM) program[21] (ICM-VLS) has previously been applied to identify new leads for a number of targets.[22,23] In the present study, the VLS docking correctly predicted seven ligands as having a higher binding affinity to ABCC5 than sildenafil. The most potent compounds, compounds **1** and **2**, showed $K_i$ of 50 −100 nM. As far as we know, these are the most potent inhibitors described for ABCC5.

Both compounds **1** and **2** feature a salicylic acid moiety, and the $pK_a$ of salicylic acid is 2.97. At physiological pH, the carboxylic acid moiety of salicylic acids tends to be negatively charged, and docking indicated that these compounds oriented the negatively charged $COO^-$ group toward Lys448 (TMH6). This ionic interaction may explain why these two compounds were the most potent ABCC5 inhibitors. The characteristic interaction of the guanine-like ring of the ligands with Gln190 (TMH1) of ABCC5, which was found in most predicted complexes, has also been observed in X-ray crystal structures of PDE5 complexed with either guanosine monophosphate (GMP) or sildenafil. In these complexes, the guanine ring of GMP, or the guanine-like ring of sildenafil, has hydrogen bond interactions with a glutamine (Gln817).[24]

The drug binding pocket of the ABCC5 model featured several polar amino acids (Gln190 (TMH1), Asn441 and Thr444 (TMH6), and Ser872 (TMH7)) and a positively charged amino acid (Lys448 (TMH6)), contributing to a molecular environment favorable for transport of organic anions. ABCC5 has been shown to transport cGMP with high affinity ($K_m$ = 2.1 $\mu M$),[5] and we have previously restored ATP-dependent cGMP transport into proteoliposomes by membrane proteins from human erythrocytes[25] and cGMP-induced ATPase activity.[25] At physiological intracellular cGMP concentration there are a number of leads that indicate ABCC5 as a high affinity and selective transporter for cGMP.[26] In the present study, the observed cGMP $K_m$ of 2.2 $\mu M$ is in agreement with the $K_m$ of 2.1 $\mu M$ reported earlier.[5] The observation from the binding affinity studies of order of potency of the known ABCC5

inhibitors sildenafil, zaprinast, and dipyridamole, with zaprinast and dipyridamole being equally potent and both being more potent than sildenafil, was also in agreement with previous observations.[27]

In the present VLS study, it was observed that each ligand had a tendency to prefer two main orientations, one toward Gln190 (in TMH1, corresponding to Leu65 (ABCB1)) and one toward Val253 (in TMH5, corresponding to Ile306 (ABCB1)). The differences in binding energy between different orientations of the same ligand did not differ significantly. This is in accordance with a study on ABCB1 where cysteine-scanning mutagenesis and reaction with a methanethiosulfonate (MTS) thiol reactive analogue of verapamil (MTS verapamil) showed that mutants Leu65Cys (TMH1) and Ile306Cys (TMH5) modified with MTS verapamil have slightly different characteristics, indicating that the bound verapamil molecules in these mutants have different orientations and that the protein can function quite well with the substrate bound in different orientations.[28] Theoretically, even though 10 different conformations of each ligand were evaluated by ICM during VLS, focusing on only the ligand orientation with best score may lead to missing out better inhibitors oriented in a pose yielding a poorer score.

Despite more than 30 years of research and development of drugs for use in co-therapy to chemotherapeutic drugs to overcome multidrug resistance (MDR), these drugs have come no further than to late-phase clinical trials.[29] The possible roles of PDE5 inhibitors in overcoming MDR is currently gaining attention as emerging evidence indicates that sildenafil and sildenafil-like drugs may enhance the sensitivity of certain tumor cells to chemotherapeutic drugs. It has also been demonstrated that sildenafil also inhibits the activity of ABC transporters such as ABCB1 and ABCG2, reversing MDR in cancer cells mediated by these transporters.[30] In the present study, we chose to use a sildenafil substructure in order to achieve compounds for VLS instead of using substructures of the slightly more potent zaprinast and dipyridamole. Zaprinast has been unsuccessful in clinical trials, and both zaprinast and dipyridamole are less selective than sildenafil.[31] Very close analogues of sildenafil were considered in this study, and even though the search pattern used for finding sildenafil analogues was the ring system in Figure 5A, the 11 compounds that were selected for testing all have much more overlap with sildenafil than the ring system in Figure 5A. Vendors presumably have generated libraries around the drug, and the additional drug-likeness filter could have biased the tested compounds even more toward close analogues of sildenafil. The ABCC5 model could also have been used to search for molecules that could not be trivially found from the starting sildenafil substructure, possibly discovering entirely new chemical scaffolds, but since sildenafil is a very interesting molecule in regard to MDR, the goal in this study was to create chemical diversity around sildenafil.

The IOV method is very time-consuming, so using the ABCC5 model as a an additional filter to select compounds to test for binding to ABCC5 in vitro, instead of testing all 105 compounds, may have saved time and lab resources. The structural and computational guidance used in the present study aided the identification of seven compounds having higher effect on cGMP efflux effect than sildenafil. The sildenafil-like hits compounds from the VLS in the present study may represent candidates for lead optimization in the search for novel drugs that can be used to overcome MDR. Such drugs may also be used to inhibit cGMP efflux from cancer cells, possibly enhancing the body's own defense mechanism of increasing cGMP levels.

Coordinates of the ABCC5 model are available upon request.

## ■ EXPERIMENTAL SECTION

**Software.** The ICM program,[21] version 3.6-1e, was used for homology modeling, compound docking, and sildenafil substructure search. The ICM program package included the ICM VLS add-on and access to Molcart, a database of chemical structures for ~4 M of commercially available compounds.

**Chemicals.** cGMP was from Sigma Aldrich (St. Louis, MO, U.S.). 8[³H]cGMP was from Perkin-Elmer (Boston, MA, U.S.). Sildenafil was a kind gift from Pfizer Inc. (NY, U.S.), and 11 compounds based on VLS were purchased from Ambinter (c/o Greenpharma SAS, 3, Allée du Titane, 45100 Orléans, France). Other chemicals were of analytical grade.

**Homology Modeling.** A multiple sequence alignment of mouse ABCB1 (SWISS-PROT accession number P06795), human ABCB1 (SWISS-PROT accession number P08183), human ABCC4 (SWISS-PROT accession number O15439), human ABCC5 (SWISS-PROT accession number O15440), human ABCC11 (SWISS-PROT accession number Q9BX80), *Escherichia coli* MsbA (SWISS-PROT accession number P60752), and *Vibrio cholerae* MsbA (Q9KQW9) was generated using T-COFFEE,[32] version 4.71 (http://tcoffee.vital-it.ch/cgi-bin/Tcoffee/tcoffee_cgi/index.cgi), and used to guide the input alignment (Figure 4) for the homology modeling.

The ABCC5 model was constructed using the X-ray crystal structure of the *Mus musculus* ABCB1[15] (PDB code 3G60), complexed with the ligand cyclic-tris-(*R*)-valineselenazole (QZ59-RRR), as a template. The ICM homology modeling module constructs the molecular model by homology from core sections defined by the average C-α atom positions in conserved regions. Loops were automatically constructed in the ICM homology module by selecting the best-fitting loop based on calculating maps around loops that were retrieved from the PDB[33] and matched in regard to sequence similarity and steric interactions with the surroundings of the model and scoring of their relative energies. The loop connecting NBD1 and TMD2 in the template, which is missing in the template, was included in the loop search procedure.

The ABCC5 model was refined by globally optimizing side chain positions and annealing the backbone using the RefineModel macro of ICM. The RefineModel macro includes (1) a side chain conformational sampling using "Montecarlo fast",[34] (2) five iterative annealings of the backbone with tethers, and (3) a second side chain conformational sampling using "Montecarlo fast". In "Montecarlo fast", the conformational space of a molecule is sampled with the ICM global optimization procedure. An iteration of the procedure, which consists of a random move followed by a local energy minimization and calculation of the complete energy, is accepted or rejected based on energy and temperature. Tethers in the iterative annealings of the backbone are harmonic restraints pulling an atom in the model to a static point in space represented by a corresponding atom in the template. The RefineModel macro was followed by the "Regul" option of ICM. "Regul", which denotes "regularization", is a procedure for fitting a protein model with the ideal covalent geometry of the residues.

The refined ABCC5 model was energy minimized using the leaprc.ff03 force field of the AMBER 9 program package.[35] Two energy minimizations were performed: (1) with restrained backbone by 500 cycles of the steepest descent minimization followed by 500 steps of conjugate gradient minimization and (2) with no restraints by 1000 cycles of the steepest descent minimization followed by 1500 steps of conjugate gradient minimization. A 10 Å cutoff radius for nonbonded interactions and a dielectric multiplicative constant of 1.0 for the electrostatic interactions were used in the molecular mechanics calculations.

The stereochemical quality of the ABCC5 model was checked using the SAVES metaserver for analyzing and validating protein structures, http://nihserver.mbi.ucla.edu/SAVES/. Programs run were Procheck,[36] What_check,[37] and Errat.[38]

**4D VLS Docking.** In order to investigate putative ligand binding modes in the highly flexible transporter protein, energy-based torsional sampling was used to generate additional conformations of the ligand binding area of ABCC5. This computational technique called "fumigation"[39] is aimed at generating more "druggable" conformations of ligand binding pockets. Fumigation is based on torsional sampling of the binding pocket side chains in the presence of a repulsive density representing a generic ligand, using the ICM biased probability Monte Carlo sampling procedure. The pocket used for torsional sampling was defined using the ligand skin mesh of QZ59-RRR from the template.[15]

In order to get a threshold score for the VLS, known binders to ABCC5 were docked using 4D docking. Thus, the VLS threshold was based scores calculated by docking sildenafil, MK571, glibenclamide, sulfinpyrazone, trequinsin, benzbromarone, verapamil, zaprinast, dipyridamole, probenecid, and cGMP. Ligands were prepared in the ICM ligand editor and converted to 3D when setting up the ligand during the docking session. Charges were also assigned in this step. A 4D docking procedure was used employing the binding pocket conformational ensembles. In this approach, the pocket ensemble conformations are used as an extra, fourth dimension of the ligand sampling space, allowing ligand docking to the multiple binding pocket conformations in a single docking simulation.[40] The three binding pocket conformations with the lowest energy were used in the 4D docking procedure.

The Molcart chemical management system, featuring a number of compound databases (including Ambinter, Chembrigde, Lifechemicals, etc.) that can be analyzed and searched using ICM cheminformatic tools, was used to retrieve compounds with a common substructure as in sildenafil (Figure 5). This substructure is a guanine-like moiety resembling the guanine part of cGMP. A database of 105 sildenafil-like compounds was obtained and used for a 4D VLS docking into the ABCC5 transporter. ICM-VLS, which is a combination of internal coordinate docking methodology and global optimization scheme, provides empirically adjusted scoring functions and accurate and fast potentials, yielding efficient virtual screening methodology in which ligands are fully and continuously flexible. Eleven hits with scores above the score threshold were selected based on the druglikeness score and ordered from Ambinter (http://www.ambinter.com/) for in vitro testing. The ICM druglikeness score is predicted based on 5000 marketed drugs from the World Drug Index (WDI) (positives) and 10 000 nondrug compounds (negatives).

**Preparation of IOV.** In the present study, a modified version of the Steck IOV preparation[41] was used. Fresh human EDTA blood was used to produce IOVs from human erythrocytes. All steps after collecting the blood were performed at 0−4 °C. The cells were sedimented by centrifugation at 2300g for 15 min. Plasma and buffycoat were discarded, and the red blood cells were washed 3 times by centrifugation at 1000g with 5 mM Tris-HCl, 113 mM KCl, pH 8.1. Cells were lysed in 10 volumes of 5 mM Tris-HCl, 0.5 mM EGTA, 4 mM KCl, pH 8.1, and washed by repeated centrifugation at 20000g for 20 min and resuspension in the same buffer until ghosts were milky white. Vesiculation was initiated by adding 39 volumes of 500 nM Tris-HCl, pH 8.2, to 1 volume of cell suspension. The vesiculation was completed by homogenization of vesicles and unsealed ghosts by passing the suspension five times through a 27G cannula. IOVs, right-side out vesicles, and unsealed vesicles and ghosts were separated by ultracentrifugation (100000g) overnight using a density gradient from 1.048 to 1.146 g/mL Histodenz (Sigma-Aldrich, St. Louis, MO, U.S.) in 5 mM Tris, 3 mM KCl, 0.3 mM EGTA. The uppermost band was collected, washed, and resuspended in 1.47 mM KH₂PO₄, 81 mM K₂HPO₄, and 140 mM KCl, pH 7.6. Sidedness was verified using acetylcholinesterase accessibility.

**Transport Assay.** cGMP is transported out of cells via ABCC5 with a $K_m$ of 2.1 μM.[5] In the present study cGMP uptake into IOVs was determined for an inhibitor concentration range of 0−320 μM, and the [³H]cGMP transport was characterized with a $K_m$ of 2.2 ± 0.35 μM. IOVs were incubated for 60 min with or without 2.0 mM ATP in a mixture containing 20 mM Tris-HCl, 10 mM MgCl₂, 1 mM EGTA, 2 μM [³H]-labeled cGMP, 121 mM KCl, pH 8.0, at 37 °C and inhibitor in a concentration range from 0 to 316 μM.
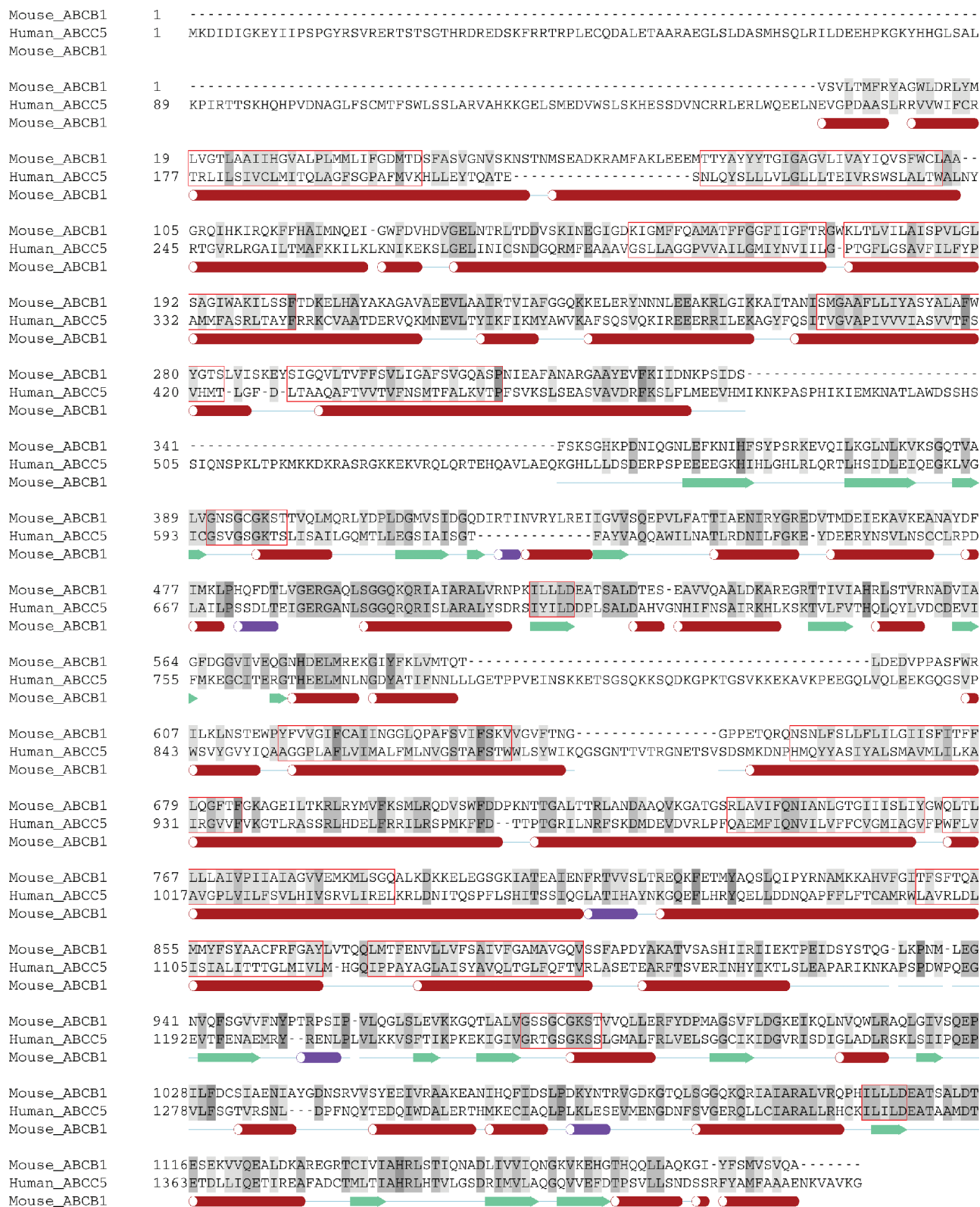
```
Mouse_ABCB1     1    ----------------------------------------------------------------------------------------
Human_ABCC5     1    MKDIDIGKEYIIPSPGYRSVRERTSTSGTHRDREDSKFRRTRPLECQDALETAARAEGLSLDASMHSQLRILDEEHPKGKYHHGLSAL
Mouse_ABCB1

Mouse_ABCB1     1    -----------------------------------------------------------------------VSVLTMFRYAGWLDRLYM
Human_ABCC5     89   KPIRTTSKHQHPVDNAGLFSCMTFSWLSSLARVAHKKGELSMEDVWSLSKHESSDVNCRRLERLWQEELNEVGPDAASLRRVVWIFCR
Mouse_ABCB1

Mouse_ABCB1     19   LVGTLAAIIHGVALPLMMLIFGDMTDSFASVGNVSKNSTNMSEADKRAMFAKLEEEMTTYAYYYTGIGAGVLIVAYIQVSFWCLAA--
Human_ABCC5     177  TRLILSIVCLMITQLAGFSGPAFMVKHLLEYTQATE-------------------SNLQYSLLLVLGLLLTEIVRSWSLALTWALNY
Mouse_ABCB1

Mouse_ABCB1     105  GRQIHKIRQKFFHAIMNQEI-GWFDVHDVGELNTRLTDDVSKINEGIGDKIGMFFQAMATFFGGFIIGFTRGWKLTLVILAISPVLGL
Human_ABCC5     245  RTGVRLRGAILTMAFKKILKLKNIKEKSLGELINICSNDGQRMFEAAAVGSLLAGGPVVAILGMIYNVIILG-PTGFLGSAVFILFYP
Mouse_ABCB1

Mouse_ABCB1     192  SAGIWAKILSSFTDKELHAYAKAGAVAEEVLAAIRTVIAFGGQKKELERYNNNLEEAKRLGIKKAITANISMGAAFLLIYASYALAFW
Human_ABCC5     332  AMMFASRLTAYFRRKCVAATDERVQKMNEVLTYIKFIKMYAWVKAFSQSVQKIREEERRILEKAGYFQSITVGVAPIVVVIASVVTFS
Mouse_ABCB1

Mouse_ABCB1     280  YGTSLVISKEYSIGQVLTVFFSVLIGAFSVGQASPNIEAFANARGAAYEVFKIIDNKPSIDS--------------------------
Human_ABCC5     420  VHMT-LGF-D-LTAAQAFTVVTVFNSMTFALKVTPFSVKSLSEASVAVDRFKSLFLMEEVHMIKNKPASPHIKIEMKNATLAWDSSHS
Mouse_ABCB1

Mouse_ABCB1     341  --------------------------------------------FSKSGHKPDNIQGNLEFKNIHFSYPSRKEVQILKGLNLKVKSGQTVA
Human_ABCC5     505  SIQNSPKLTPKMKKDKRASRGKKEKVRQLQRTEHQAVLAEQKGHLLLLDSDERPSPEEEEGKHIHLGHLRLQRTLHSIDLEIQEGKLVG
Mouse_ABCB1

Mouse_ABCB1     389  LVGNSGCGKSTTVQLMQRLYDPLDGMVSIDGQDIRTINVRYLREIIGVVSQEPVLFATTIAENIRYGREDVTMDEIEKAVKEANAYDF
Human_ABCC5     593  ICGSVGSGKTSLISAILGQMTLLEGSIAISGT-------------FAYVAQQAWILNATLRDNILFGKE-YDEERYNSVLNSCCLRPD
Mouse_ABCB1

Mouse_ABCB1     477  IMKLPHQFDTLVGERGAQLSGGQKQRIAIARALVRNPKILLLDEATSALDTES-EAVVQAALDKAREGRTTIVIAHRLSTVRNADVIA
Human_ABCC5     667  LAILPSSDLTEIGERGANLSGGQRQRISLARALYSDRSIYILDDPLSALDAHVGNHIFNSAIRKHLKSKTVLFVTHQLQYLVDCDEVI
Mouse_ABCB1

Mouse_ABCB1     564  GFDGGVIVEQGNHDELMREKGIYFKLVMTQT------------------------------------------------LDEDVPPASFWR
Human_ABCC5     755  FMKEGCITERGTHEELMNLNGDYATIFNNLLLGETPPVEINSKKETSGSQKKSQDKGPKTGSVKKEKAVKPEEGQLVQLEEKGQGSVP
Mouse_ABCB1

Mouse_ABCB1     607  ILKLNSTEWPYFVVGIFCAIINGGLQPAFSVIFSKVVGVFTNG----------------GPPETQRQNSNLFSLLFLILGIISFITFF
Human_ABCC5     843  WSVYGVYIQAAGGPLAFLVIMALFMLNVGSTAFSTWWLSYWIKQGSGNTTVTRGNETSVSDSMKDNPHMQYYASIYALSMAVMLILKA
Mouse_ABCB1

Mouse_ABCB1     679  LQGFTFGKAGEILTKRLRYMVFKSMLRQDVSWFDDPKNTTGALTTRLANDAAQVKGATGSRLAVIFQNIANLGTGIIISLIYGWQLTL
Human_ABCC5     931  IRGVVFVKGTLRASSRLHDELFRRILRSPMKFFD--TTPTGRILNRFSKDMDEVDVRLPFQAEMFIQNVILVFFCVGMIAGVFPWFLV
Mouse_ABCB1

Mouse_ABCB1     767  LLLAIVPIIAIAGVVEMKMLSGQALKDKKELEGSGKIATEAIENFRTVVSLTREQKFETMYAQSLQIPYRNAMKKAHVFGITFSFTQA
Human_ABCC5     1017 AVGPLVILFSVLHIVSRVLIRELKRLDNITQSPFLSHITSSIQGLATIHAYNKGQEFLHRYQELLDDNQAPFFLFTCAMRWLAVRLDL
Mouse_ABCB1

Mouse_ABCB1     855  MMYFSYAACFRFGAYLVTQQLMTFENVLLVFSAIVFGAMAVGQVSSFAPDYAKATVSASHIIRIIEKTPEIDSYSTQG-LKPNM-LEG
Human_ABCC5     1105 ISIALITTTGLMIVLM-HGQIPPAYAGLAISYAVQLTGLFQFTVRLASETEARFTSVERINHYIKTLSLEAPARIKNKAPSPDWPQEG
Mouse_ABCB1

Mouse_ABCB1     941  NVQFSGVVFNYPTRPSIP-VLQGLSLEVKKGQTLALVGSSGCGKSTVVQLLERFYDPMAGSVFLDGKEIKQLNVQWLRAQLGIVSQEP
Human_ABCC5     1192 EVTFENAEMRY--RENLPLVLKKVSFTIKPKEKIGIVGRTGSGKSSLGMALFRLVELSGGCIKIDGVRISDIGLADLRSKLSIIPQEP
Mouse_ABCB1

Mouse_ABCB1     1028 ILFDCSIAENIAYGDNSRVVSYEEIVRAAKEANIHQFIDSLPDKYNTRVGDKGTQLSGGQKQRIAIARALVRQPHILLLDEATSALDT
Human_ABCC5     1278 VLFSGTVRSNL---DPFNQYTEDQIWDALERTHMKECIAQLPLKLESEVMENGDNFSVGERQLLCIARALLRHCKILILDEATAAMDT
Mouse_ABCB1

Mouse_ABCB1     1116 ESEKVVQEALDKAREGRTCIVIAHRLSTIQNADLIVVIQNGKVKEHGTHQQLLAQKGI-YFSMVSVQA-------
Human_ABCC5     1363 ETDLLIQETIREAFADCTMLTIAHRLHTVLGSDRIMVLAQGVVEFDTPSVLLSNDSSRFYAMFAAAENKVAVKG
Mouse_ABCB1
```

**Figure 4.** Alignment of mouse ABCB1 and human ABCC5 used as input alignment for the ICM homology modeling module. TMHs are indicated as boxes. Secondary structure of template is indicated as follows: $\alpha$ helix = red cylinder; $3_{10}$ helix = purple cylinder; $\beta$ sheet = green arrow.

The transport process was stopped with addition of ice-cold 1.47 mM KH$_2$PO$_4$, 8.1 mM K$_2$HPO$_4$, and 140 mM KCl, pH 7.6. The IOVs were separated from the incubation medium by filtration (nitrocellulose membrane, 0.22 $\mu$m GSWP, Millipore, Billerica, MA, U.S.). The radioactivity on the filters was quantified by liquid scintillation (Ultima Gold XR, Packard, Groningen, The Netherlands) in a Packard 1900 TR liquid scintillation analyzer. DMSO was needed to dissolve some of the inhibitors and was added to a similar concentration in the control samples (without inhibitors).
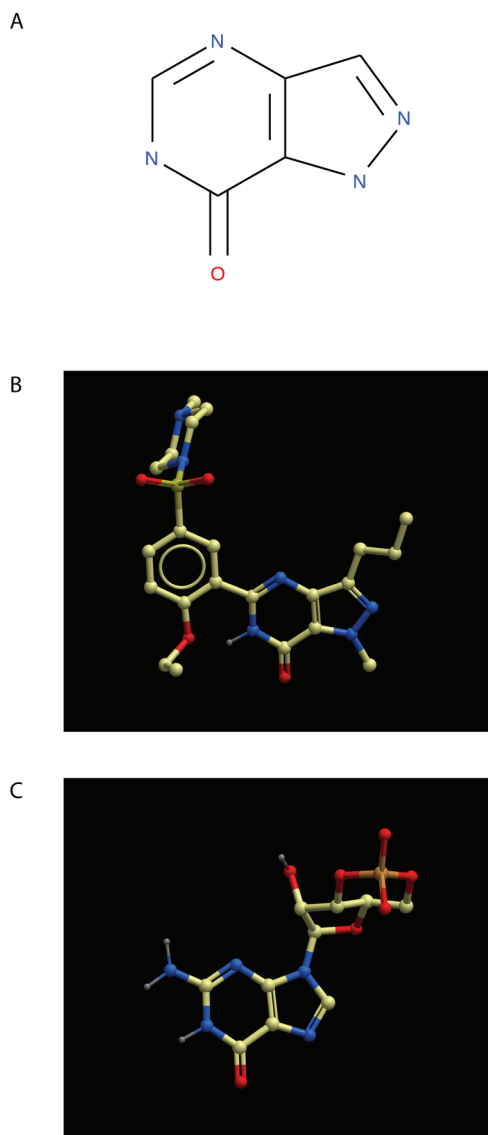
A



B



C



**Figure 5.** (A) Sildenafil substructure used to retrieve sildenafil-like compounds from Molcart. (B) Molecular structure of sildenafil. (C) Molecular structure of cGMP.

**Determination of $K_i$ Values.** The $IC_{50}$ values were determined and transformed to $K_i$ values according to Cheng and Prusoff.[42]

**Statistics.** The results are presented as mean value ± SEM. Unpaired two-tailed $t$ test with Welch correction was performed using GraphPad InStat, version 3.06, GraphPad Software, San Diego, CA, U.S.

## AUTHOR INFORMATION

**Corresponding Author**
*Phone: +4777644706. E-mail: Aina.W.Ravna@uit.no.

**Notes**
The authors declare no competing financial interest.

## ACKNOWLEDGMENTS

## ABBREVIATIONS USED

ABC, ATP binding cassette; cGMP, cyclic guanosine monophosphate; GMP, guanosine monophosphate; ICM, internal coordinate mechanics; ICM-VLS, virtual ligand screening add-on to the internal coordinate mechanics program; IOV, inside-out vesicles; MDR, multidrug resistance; MTS, methanethiosulfonate; NBD, nucleotide binding domain; PDE5, phosphodiesterase 5; SAVES, stuctural analysis and verification server; TMD, transmembrane domain; TMH, transmembrane helix; VLS, virtual ligand screening; WDI, World Drug Index

## REFERENCES

(1) Luesley, D. M.; Blackledge, G. R.; Chan, K. K.; Newton, J. R. Random urinary cyclic 3′,5′ guanosine monophosphate in epithelial ovarian cancer: relation to other prognostic variables and to survival. *Br. J. Obstet. Gynaecol.* **1986**, *93*, 380−385.

(2) Orbo, A.; Jaeger, R.; Sager, G. Urinary levels of cyclic guanosine monophosphate (cGMP) in patients with cancer of the uterine cervix: a valuable prognostic factor of clinical outcome? *Eur. J. Cancer* **1998**, *34*, 1460−1462.

(3) Peracchi, M.; Bamonti-Catena, F.; Lombardi, L.; Toschi, V.; Bareggi, B.; Cortelezzi, A.; Maiolo, A. T.; Polli, E. E. Plasma cyclic nucleotide levels in monitoring acute leukemia patients. *Cancer Detect. Prev.* **1985**, *8*, 291−295.

(4) Turner, G. A.; Greggi, S.; Guthrie, D.; Benedetti Panici, P.; Ellis, R. D.; Scambia, G.; Mancuso, S. Monitoring ovarian cancer using urine cyclic GMP. A two-centre study. *Eur. J. Gynaecol. Oncol.* **1990**, *11*, 421−427.

(5) Jedlitschky, G.; Burchell, B.; Keppler, D. The multidrug resistance protein 5 functions as an ATP-dependent export pump for cyclic nucleotides. *J. Biol. Chem.* **2000**, *275*, 30069−30074.

(6) Pilz, R. B.; Broderick, K. E. Role of cyclic GMP in gene regulation. *Front. Biosci.* **2005**, *10*, 1239−1268.

(7) Saier, M. H. Jr. A functional-phylogenetic classification system for transmembrane solute transporters. *Microbiol. Mol. Biol. Rev.* **2000**, *64*, 354−411.

(8) Dean, M.; Rzhetsky, A.; Allikmets, R. The human ATP-binding cassette (ABC) transporter superfamily. *Genome Res.* **2001**, *11*, 1156−1166.

(9) Ravna, A. W.; Sylte, I.; Sager, G. Molecular model of the outward facing state of the human P-glycoprotein (ABCB1), and comparison to a model of the human MRP5 (ABCC5). *Theor. Biol. Med. Modell.* **2007**, *4*, 33.

(10) Ravna, A. W.; Sylte, I.; Sager, G. Binding site of ABC transporter homology models confirmed by ABCB1 crystal structure. *Theor. Biol. Med. Modell.* **2009**, *6*, 20.

(11) Ravna, A. W.; Sager, G. Molecular model of the outward facing state of the human multidrug resistance protein 4 (MRP4/ABCC4). *Bioorg. Med. Chem. Lett.* **2008**, *18*, 3481−3483.

(12) Ravna, A. W.; Sylte, I.; Sager, G. A molecular model of a putative substrate releasing conformation of multidrug resistance protein 5 (MRP5). *Eur. J. Med. Chem.* **2008**, *43*, 2557−2567.

(13) Dawson, R. J.; Locher, K. P. Structure of a bacterial multidrug ABC transporter. *Nature* **2006**, *443*, 180−185.

(14) Ward, A.; Reyes, C. L.; Yu, J.; Roth, C. B.; Chang, G. Flexibility in the ABC transporter MsbA: alternating access with a twist. *Proc. Natl. Acad. Sci. U.S.A.* **2007**, *104*, 19005−19010.

(15) Aller, S. G.; Yu, J.; Ward, A.; Weng, Y.; Chittaboina, S.; Zhuo, R.; Harrell, P. M.; Trinh, Y. T.; Zhang, Q.; Urbatsch, I. L.; Chang, G. Structure of P-glycoprotein reveals a molecular basis for poly-specific drug binding. *Science* **2009**, *323*, 1718−1722.

(16) Beuming, T.; Shi, L.; Javitch, J. A.; Weinstein, H. A comprehensive structure-based alignment of prokaryotic and eukaryotic neurotransmitter/Na⁺ symporters (NSS) aids in the use of the LeuT structure to probe NSS structure and function. *Mol. Pharmacol.* **2006**, *70*, 1630−1642.

(17) Hibert, M. F.; Trumpp-Kallmeyer, S.; Bruinvels, A.; Hoflack, J. Three-dimensional models of neurotransmitter G-binding protein-coupled receptors. *Mol. Pharmacol.* **1991**, *40*, 8−15.

(18) Loo, T. W.; Bartlett, M. C.; Clarke, D. M. Human P-glycoprotein is active when the two halves are clamped together in the

closed conformation. *Biochem. Biophys. Res. Commun.* **2010**, *395*, 436−440.

(19) Verhalen, B.; Wilkens, S. P-glycoprotein retains drug-stimulated ATPase activity upon covalent linkage of the two nucleotide binding domains at their C-terminal ends. *J. Biol. Chem.* **2011**, *286*, 10476−10482.

(20) Loo, T. W.; Bartlett, M. C.; Clarke, D. M. Substrate-induced conformational changes in the transmembrane segments of human P-glycoprotein. Direct evidence for the substrate-induced fit mechanism for drug binding. *J. Biol. Chem.* **2003**, *278*, 13603−13606.

(21) Abagyan, R.; Totrov, M.; Kuznetsov, D. N. ICM: a new method for protein modeling and design. Applications to docking and structure prediction from the distorted native comformation. *J. Comput. Chem.* **1994**, *15*, 488−506.

(22) Cavasotto, C. N.; Orry, A. J.; Murgolo, N. J.; Czarniecki, M. F.; Kocsi, S. A.; Hawes, B. E.; O'Neill, K. A.; Hine, H.; Burton, M. S.; Voigt, J. H.; Abagyan, R. A.; Bayne, M. L.; Monsma, F. J. Jr. Discovery of novel chemotypes to a G-protein-coupled receptor through ligand-steered homology modeling and structure-based virtual screening. *J. Med. Chem.* **2008**, *51*, 581−588.

(23) Katritch, V.; Byrd, C. M.; Tseitin, V.; Dai, D.; Raush, E.; Totrov, M.; Abagyan, R.; Jordan, R.; Hruby, D. E. Discovery of small molecule inhibitors of ubiquitin-like poxvirus proteinase I7L using homology modeling and covalent docking approaches. *J. Comput.-Aided Mol. Des.* **2007**, *21*, 549−558.

(24) Zhang, K. Y.; Card, G. L.; Suzuki, Y.; Artis, D. R.; Fong, D.; Gillette, S.; Hsieh, D.; Neiman, J.; West, B. L.; Zhang, C.; Milburn, M. V.; Kim, S. H.; Schlessinger, J.; Bollag, G. A glutamine switch mechanism for nucleotide selectivity by phosphodiesterases. *Mol. Cell* **2004**, *15*, 279−286.

(25) Boadu, E.; Sager, G. ATPase activity and transport by a cGMP transporter in human erythrocyte ghosts and proteoliposome-reconstituted membrane extracts. *Biochim. Biophys. Acta* **2000**, *1509*, 467−474.

(26) Sager, G.; Ravna, A. W. Cellular efflux of cAMP and cGMP: a question about selectivity. *Mini-Rev. Med. Chem.* **2009**, *9*, 1009−1013.

(27) Sundkvist, E.; Jaeger, R.; Sager, G. Pharmacological character-ization of the ATP-dependent low K(m) guanosine 3′,5′-cyclic monophosphate (cGMP) transporter in human erythrocytes. *Biochem. Pharmacol.* **2002**, *63*, 945−949.

(28) Loo, T. W.; Bartlett, M. C.; Clarke, D. M. Transmembrane segment 1 of human P-glycoprotein contributes to the drug-binding pocket. *Biochem. J.* **2006**, *396*, 537−545.

(29) Wu, C. P.; Calcagno, A. M.; Ambudkar, S. V. Reversal of ABC drug transporter-mediated multidrug resistance in cancer cells: evaluation of current strategies. *Curr. Mol. Pharmacol.* **2008**, *1*, 93−105.

(30) Shi, Z.; Tiwari, A. K.; Patel, A. S.; Fu, L. W.; Chen, Z. S. Roles of sildenafil in enhancing drug sensitivity in cancer. *Cancer Res.* **2011**, *71*, 3735−3738.

(31) Kulkarni, S. K.; Patil, C. S. Phosphodiesterase 5 enzyme and its inhibitors: update on pharmacological and therapeutical aspects. *Methods Find. Exp. Clin. Pharmacol.* **2004**, *26*, 789−799.

(32) Notredame, C.; Higgins, D. G.; Heringa, J. T-Coffee: a novel method for fast and accurate multiple sequence alignment. *J. Mol. Biol.* **2000**, *302*, 205−217.

(33) Berman, H. M.; Westbrook, J.; Feng, Z.; Gilliland, G.; Bhat, T. N.; Weissig, H.; Shindyalov, I. N.; Bourne, P. E. The Protein Data Bank. *Nucleic Acids Res.* **2000**, *28*, 235−242.

(34) Abagyan, R.; Totrov, M. Biased probability Monte Carlo conformational searches and electrostatic calculations for peptides and proteins. *J. Mol. Biol.* **1994**, *235*, 983−1002.

(35) Case, D. A.; Darden, T. A.; Cheatham, T. E., III; Simmerling, C. L.; Wang, J.; Duke, R. E.; Luo, R.; Merz, K. M.; Pearlman, D. A.; Crowley, M.; Walker, R. C.; Zhang, W.; Wang, B.; Hayik, A.; Roitberg, A.; Seabra, G.; Wong, K.; Paesani, F.; Wu, X.; Brozell, S.; Tsui, V.; Gohlke, H.; Yang, L.; Tan, C.; Mongan, J.; Hornak, V.; Cui, G.; Beroza, P.; Mathews, D. H.; Schafmeister, C.; Ross, W. S.; Kollman, P. A. *AMBER 9*; University of California: San Francisco, CA, 2006.

(36) Laskoswki, R. A.; MacArthur, M. W.; Moss, D. S.; Thorton, J. M. PROCHECK: a program to check the stereochemical quality of protein structures. *J. Appl. Crystallogr.* **1993**, *26*, 283−291.

(37) Hooft, R. W.; Vriend, G.; Sander, C.; Abola, E. E. Errors in protein structures. *Nature* **1996**, *381*, 272.

(38) Colovos, C.; Yeates, T. O. Verification of protein structures: patterns of nonbonded atomic interactions. *Protein Sci.* **1993**, *2*, 1511−1519.

(39) Abagyan, R.; Kufareva, I. The flexible pocketome engine for structural chemogenomics. *Methods Mol. Biol.* **2009**, *575*, 249−279.

(40) Bottegoni, G.; Kufareva, I.; Totrov, M.; Abagyan, R. Four-dimensional docking: a fast and accurate account of discrete receptor flexibility in ligand docking. *J. Med. Chem.* **2009**, *52*, 397−406.

(41) Steck, T. L.; Weinstein, R. S.; Straus, J. H.; Wallach, D. F. Inside-out red cell membrane vesicles: preparation and purification. *Science* **1970**, *168*, 255−257.

(42) Cheng, Y.; Prusoff, W. H. Relationship between the inhibition constant (K1) and the concentration of inhibitor which causes 50% inhibition (I50) of an enzymatic reaction. *Biochem. Pharmacol.* **1973**, *22*, 3099−3108.